Journal of Applied Mechanics and Technical Physics, Vol. 50, No. 3, pp. 406–412, 2009

EXPLOSIVE PROJECTION OF LIQUID FROM A THICK-WALLED CYLINDRICAL CONTAINER

V. A. Bykov, E. F. Gryaznov, and V. N. Okhitin

UDC 621.7.044.2

The process of projection of a layer of an ideal liquid enclosed into a cylindrical elastoplastic shell by products of instantaneous detonation of a high explosive charge is studied numerically in a two-dimensional plane formulation. The processes of shell fracture and liquid exhaustion through the resultant slots are considered. Numerical results are analyzed, and analytical relations for angular distributions of radial velocity and mass of the liquid escaping through the slots are derived.

Key words: *explosion, liquid, elastoplastic shell, fracture, jet.*

The method of explosive spraying of the liquid finds applications in various areas of human activities. This method implies blasting of a high explosive (HE) charge inside a container filled by the liquid. This method is used to generate water screens in mines dangerous in terms of dust and gas [1, 2], to affect hail clouds [3], and to extinguish fires [4].

The results of studying the explosive method of liquid spraying were obtained for models with a low-strength container or without it.

In the present work, the process of projection of a layer of an ideal liquid enclosed into a cylindrical elastoplastic shell by products of instantaneous detonation of an HE charge is studied numerically in a two-dimensional plane formulation. A sketch of the model is shown in Fig. 1 (R_0, a_0, and b_0 are the initial radii of the charge, liquid layer, and shell, respectively).

Two-dimensional plane motion of the system consisting of detonation products (DPs), the liquid, and the shell was described by a combined Eulerian–Lagrangian finite-difference method for the numerical solution of the system of equations of mechanics of continuous media. The system of equations that describe two-dimensional plane motion of an elastoplastic shell in polar Eulerian coordinates in the Lagrangian form can be found, e.g., in [5].

To describe the flow in the region of the plastic state of the shell, we used the procedure of reduction of the calculated elastic stresses to the yield circle in accordance with the Mises yield condition [6]. The volume compressibility of the shell was defined in the form of the Tait equation [7].

The system of differential equations that describe a two-dimensional plane adiabatic flow of an ideal liquid and gas in polar Eulerian coordinates (r, θ) was given, for instance, in [8].

The system was supplemented with the equation of state of the media in the caloric form $p = p(\gamma, \rho, E)$, which included an additional variable γ determining the phase composition of the medium, apart from two thermodynamic parameters (density ρ and specific internal energy E). If the Eulerian grid is used, it is impossible to draw a distinct boundary between the detonation products and the liquid at any instant of time, except for the initial one; therefore, the system of equations should be supplemented with a relation for separating the phases. A certain value of γ was assigned to particles of each medium. The condition $d\gamma/dt = 0$ had to be satisfied along the trajectory of each particle. In polar Eulerian coordinates, this condition acquires the form

$$\frac{\partial \gamma}{\partial t} + u\,\frac{\partial \gamma}{\partial r} + \frac{v}{r}\,\frac{\partial \gamma}{\partial \theta} = 0,$$

where t is the time, and u and v are the radial and tangential components of the mass velocity of the medium.

Bauman Moscow State Technical University, Moscow 105005; Okhitin@sm.bmstu.ru. Translated from Prikladnaya Mekhanika i Tekhnicheskaya Fizika, Vol. 50, No. 3, pp. 56–63, May–June, 2009. Original article submitted April 3, 2008.

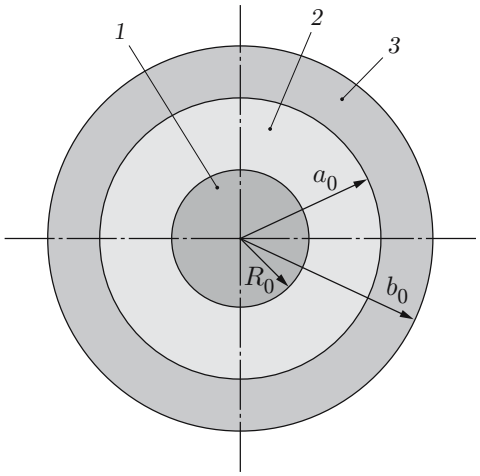

Fig. 1. Sketch of the model: 1) HE; 2) liquid; 3) shell.

For convenience of calculations, we assumed that $\gamma = 0$ for the liquid and $\gamma = 1$ for the detonation products. Then, using the Tait equation for the liquid

$$p_l = B_l[(\rho_l/\rho_{l0})^{m_l} - 1],$$

and the Mie–Grüneisen equation for the detonation products [9]

$$p_g = C\rho_g^{m_g} + \Gamma E \rho_g$$

(p and Γ are the pressure and the Grüneisen coefficient; B, C, and m are numerical coefficients; the subscripts l, g, and 0 refer to the liquid, gaseous detonation products, and initial state of the medium, respectively), we can write the equation for pressure in both media:

$$p = \gamma p_g + (1 - \gamma) p_l.$$

The systems of equations for the shell and for the DP–liquid region were solved together with the use of conventional initial and boundary conditions for the case of instantaneous detonation of the charge.

The condition $\sigma_n = p_w$, where p_w is the pressure in the attached air shock wave, was imposed for the normal stress on the outer surface of the shell.

The system of equations for the detonation products and the liquid was solved by an explicit two-step second-order predictor–corrector scheme on a moving Eulerian grid [10]. Numerical integration of the system of equations for the shell was performed with an explicit second-order scheme with artificial viscosity [6]. The grid size was $N_r \times N_\theta = 120 \times (40–18)$ in calculations for the detonation products and the liquid and $N_r \times N_\theta = 20 \times (80–40)$ for the shell (depending on the angle of the calculated sector).

The two-dimensional algorithm was tested through comparisons of the calculated results with the results obtained for a one-dimensional problem [11] for a model (36/64 TNT/RDX explosive with water as a filler; shell material is steel with the dynamic yield stress $Y = 1.7$ GPa) with the following parameters (see Fig. 1): $R_0 = 11$ mm, $a_0 = 20$ mm, and $b_0 =$ var; shell fracture was ignored. In the results calculated by the two-dimensional and one-dimensional algorithms, the maximum velocities of shell projection differed by less than 3–4%. In the tests, the disbalance of the total mass was within 1–2%, and the energy disbalance was 2–3%.

In a real process of shell expansion, it becomes broken into fragments by the mechanism of crack propagation. The issue of choosing the boundary condition at the tip of the crack propagating in the shell under pulsed loading is rather complicated and has not been completely solved yet. The process of fracture of a shell loaded by detonation products of a contact HE charge has been well studied. Such shells become destroyed under the joint propagation of spall cracks in the outer zone affected by tensile stresses and shear cracks in the compressed inner zone [12, 13]. Various criteria are used to describe crack propagation [14, 15].

Constructing a computational domain that allows the propagation of cracks of both types to be considered is a rather complicated problem. In addition, for shells loaded by detonation products through a liquid layer, only some

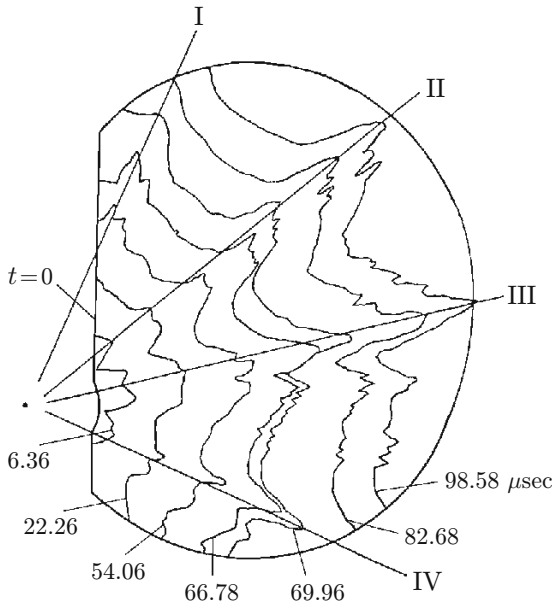

Fig. 2. Schematic presentation of results of high-speed filming of an explosion of a cylindrical model: the boundaries of the shell resolution sectors are indicated by I–IV.

particular results of experiments are available, and there are no reliable data on the mechanism of their fracture. At the same time, it seems unreasonable to ignore crack propagation (for instance, in the case of instantaneous fracture of the shell after reaching a certain radius), because the shell can experience bending in the course of reduction of the cross-sectional area because of crack propagation, which can lead to redistribution of the liquid flow inside the shell and, finally, affect the scattering parameters after shell fracture.

We used the following simplified model of crack propagation: the number of cracks (angle of the calculated sector) was set on the basis of experimental data [16]; the crack was assumed to propagate from the outer surface inward the shell under the condition of positive (tensile) tangential stresses in the vicinity of the crack tip [14]; the velocity of motion of the crack tip was determined by means of test calculations from the condition that the shell becomes completely destroyed when a certain radius (time) known from experiments [16] is reached; $\sigma_\theta = 0$ on the crack edges if it is open or is opening; if the crack edges are closed, they transfer tangential compressive stresses; at the moment when the shell becomes completely destroyed, each fragment is "frozen," i.e., the calculation of stresses inside the fragment is terminated, and the fragment is assumed to move along its plane of symmetry (along one of the computational domain boundaries) with a velocity U determined from the Newton's second law of motion $M_p\, dU/dt = \Delta p\, S_p$, where M_p and S_p are the mass and area of the part of the fragment in the computational domain, respectively, and Δp is the mean pressure difference on the inner and outer surfaces of the fragment.

The liquid can partially escape through the slots formed owing to shell fracture, which is accompanied by complex interaction of liquid particles with each other and with the ambient atmosphere. A simplified method for jet calculation is used in the present work. Liquid particles located outside the computational domain are assumed to continue their motion with a constant velocity in an unchanged direction, and they do not interact with each other. As the velocity of jet exhaustion through the slot is smaller than the velocity of sound in the liquid, a pressure equal to the counterpressure p_w is assumed to be established in the plane of the slot. Hence, the parameters in the boundary nodes of the computational grid in the region of the slot are calculated by a one-sided scheme with a boundary condition for pressure.

To check the adequacy of the proposed model of jet formation, we compared the numerical results with the data obtained by means of high-speed filming of explosions of cylindrical models [16]. The results of filming of the explosion of one model are schematically illustrated in Fig. 2. The shell radius is assumed to be the radius of depressions between the jets. At the same time instants after the beginning of shell motion, the calculated jet radius is slightly greater than that on the photographs (for the radius $7a_0$, the difference reaches 7%), while the calculated

TABLE 1

Load Factor as a Function of the Initial Parameters of the Model

R_0, mm	b_0, mm	a_f/a_0	n_θ	β
4.5	50.0	1.40	4	0.01221
8.0	32.0	1.35	12	0.03920
11.0	26.7	1.40	16	0.075 65
15.0	23.3	1.40	25	0.14620

Note. The values of R_0 were obtained for $b_0 = 26.7$ mm, and the values of b_0 were obtained for $R_0 = 11$ mm.

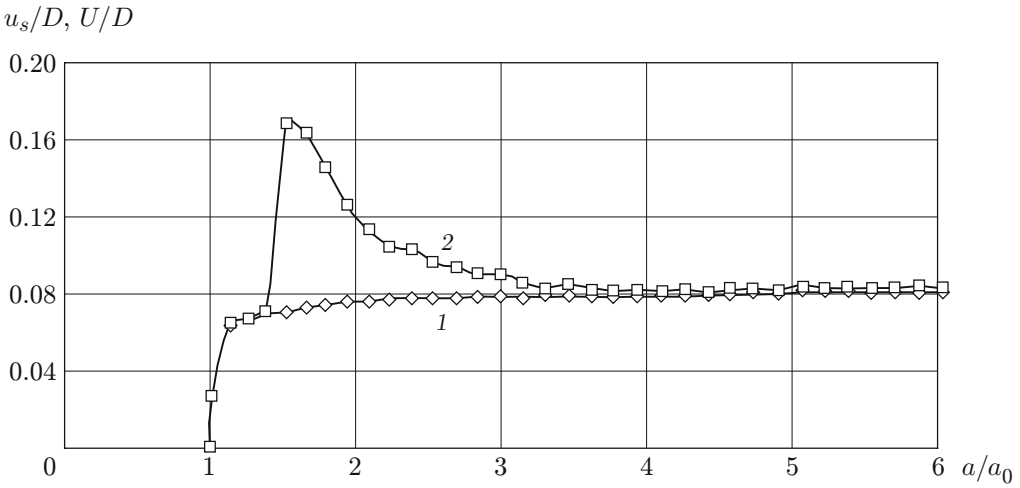

Fig. 3. Radial velocity of the shell (curve 1) and the jet (curve 2) versus the degree of shell expansion for the model with $R_0 = 11$ mm.

shell radius is slightly smaller (for the radius $5a_0$, the difference reaches 15%). The first fact can be explained by deceleration of the real jet in air. The reason for the second fact can be the liquid flow around the shell fragments. As a whole, we can conclude that the proposed model of jet calculation provides a satisfactory description of the real pattern of the explosion.

In numerical simulations, the load factor β equal to the ratio of the HE mass to the total mass of the charge and the shell in the cross section changed both owing to the change in the charge radius with unchanged radii of the liquid and the shell and owing to the change in the outer radius of the shell with unchanged radii of the liquid and the HE charge. The calculations were performed for a model (36/64 TNT/RDX explosive with water as a filler; shell material is steel with the dynamic yield stress $Y = 1.7$ GPa) with the following initial parameters: HE charge radius $R_0 = 4.5$, 8.0, 11.0, and 15.0 mm, inner radius of the shell (radius of the liquid) $a_0 = 20$ mm, outer radius of the shell $b_0 = 23.3$, 26.7, 32.0, and 50.0 mm, relative radius of shell fracture a_f/a_0, and number of segments over the shell circumference n_θ, which were borrowed from experiments [16]. The load factors obtained for these data are listed in Table 1.

Figure 3 shows the velocity of the shell U and the velocity of jet exhaustion u_s normalized to the detonation velocity D as functions of the degree of shell expansion a/a_0 for the model with the load factor $\beta = 0.07565$. The velocities of the shell and the liquid are identical until the shell fracture with formation of holes. When the inner radius of the shell reaches a certain value ($a_f/a_0 = 1.4$), the crack propagating from the outer surface of the shell separates the latter, and the liquid filler starts to exhaust through the resultant slot. The maximum velocity of jet exhaustion is more than twice the shell velocity; nevertheless, the jet velocity rapidly decreases and, as the slot becomes rather wide, becomes almost equal to the velocity of shell fragments, which increases insignificantly after the shell fracture.

The mass fraction of the liquid escaping through the slots increases with increasing load factor; for a constant value of β, the mass fraction increases with increasing charge radius and can exceed 40% in some cases.

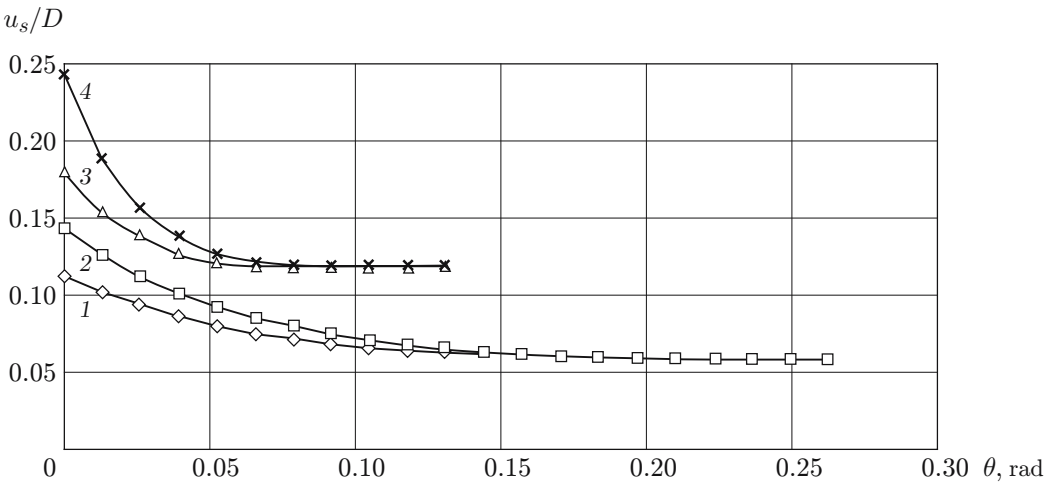

Fig. 4. Distributions of radial velocity of the exhausting jet over the angle for $\beta = 0.0392$ (curves 1 and 2) and $\beta = 0.1462$ (curves 3 and 4): 1) $R_0 = 8$ mm and $b_0 = 26.7$ mm; 2) $R_0 = 11$ mm and $b_0 = 32$ mm; 3) $R_0 = 11$ mm and $b_0 = 23.3$ mm; 4) $R_0 = 15$ mm and $b_0 = 26.7$ mm.

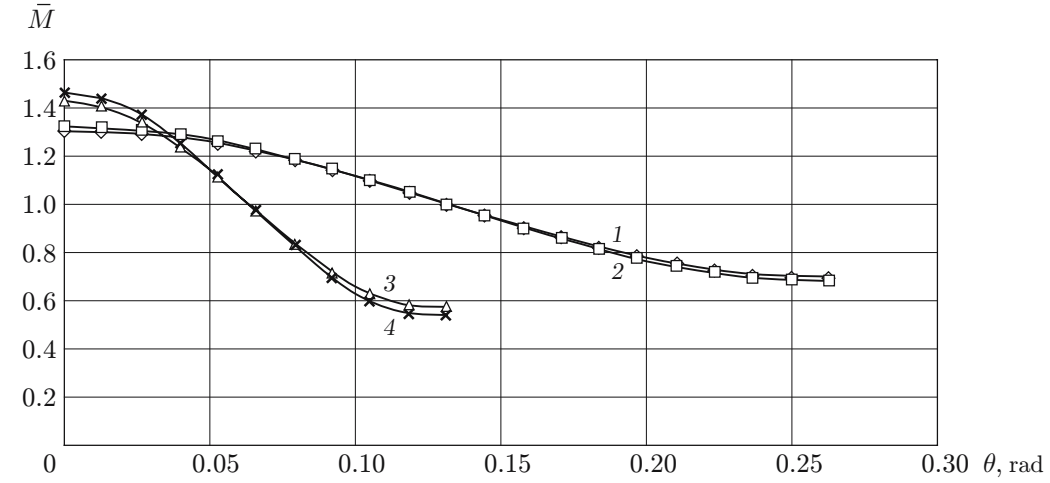

Fig. 5. Angular distribution of the liquid mass for different values of the charge and shell radii (notation the same as in Fig. 4).

Figure 4 shows the distributions of radial velocity of jet exhaustion in the course of shell expansion after its fracture over the angular coordinate inside the computational sector for two values of the load factor obtained for different combinations of the model radius (see Table 1). For identical load factors on the plane of symmetry of the crack, the maximum velocities of jet exhaustion are substantially different and increase with increasing charge radius, while these velocities in the region adjacent to the fragment are identical and almost equal to the maximum radial velocity of the shell. Depending on the load factor, the maximum velocity of jet exhaustion increases by a factor of 1.5 to 2 as the charge radius is changed from 8 to 15 mm. The maximum tangential velocity of the liquid in the jet is 10 to 20 times lower than the maximum radial velocity of jet exhaustion.

Figures 5 and 6 show the distributions of the relative mass of the liquid over the angle $\bar{M}(\theta)$ (in the computational sector) and the mass flow of the liquid through the slots as a function of the degree of shell expansion $\Delta\bar{M}(a/a_0)$ for $\beta = 0.0392$ and 0.1462 and different values of the charge and shell radii. It is seen that the nonuniformities in the angular distributions of the liquid mass and its mass flow through the slots are mainly determined by the load factor. For a constant value of β, these parameters slightly increase with increasing charge radius.

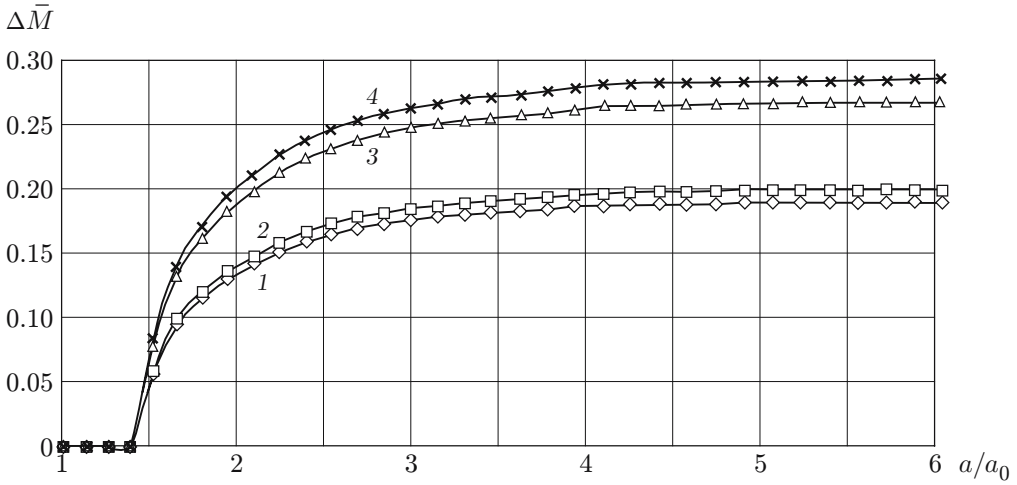

Fig. 6. Mass flow of the liquid through the slots versus the degree of shell expansion for different values of the charge and shell radii (notation the same as in Fig. 4).

An arbitrary increase in the number of sectors into which the shell is divided, other conditions being identical, leads to a certain decrease in the shell velocity and in the maximum radial velocity of jet exhaustion; the mass flow of the liquid through the slots somewhat increases thereby.

In our earlier paper [11], we proposed an analytical dependence for determining the maximum velocity of projection of a solid shell through a liquid layer

$$\frac{u_0}{D} = \frac{1}{2}\left(\frac{\beta(1-\eta_p-\eta_l)}{2+\beta}\right)^{1/2}, \tag{1}$$

where η_p and η_l are the relative energy losses due to plastic deformation of the shell and heating of the liquid on the front of shock waves.

If irreversible energy losses are ignored ($\eta_p = \eta_l = 0$), dependence (1) transforms to Pokrovskii's formula [7], which implies that the velocity of projection of the shell and the liquid is determined by the load factor only and does not depend directly on the HE charge radius. If these losses, which can exceed 25%, are taken into account [11], however, the velocity of the shell (and adjacent layers of the liquid) increases with increasing charge radius, and this increase is more pronounced for lower values of the load factor. The calculated shell velocities are 5 to 13% lower than the corresponding values predicted by the analytical formulas. A possible reason is the neglect of the decrease in velocity caused by exhaustion of some part of the liquid through the slots and by the decrease in pressure on the inner surface of the shell in analytical calculations.

Thus, we can note that the velocity of shell projection is almost completely determined by the load factor, and its value agrees well with the analytical estimate, while the jet velocity depends to a large extent on the HE charge radius at a constant load factor. For the HEs (A–IX-1, TNT with densities of 1 and 1.6 g/cm^3, and RDX of bulk density), shell materials (steel, titanium, and aluminum), and fillers (water, ethyl alcohol, and gasoline) considered in the present study, no qualitative differences were observed. Quantitative differences in the parameters of projection of the shell and the liquid filler for models with identical geometric characteristics can be attributed to different values of the load factor of materials with different densities or to different characteristics of the HEs used.

An analysis of the results obtained shows that the distributions of the radial velocity of the liquid mass over the angle varied from the plane of symmetry of the crack to the plane of symmetry of the shell fragment can be described by the following formulas:

$$\frac{u_s}{D} = \frac{u_0}{D}\{1 + F_1F_2F_3F_4F_5\exp[-(6+0.0619n_\theta^2)\theta]\}, \qquad \bar{M} = 1 + G_1G_2G_3G_4G_5\cos(\theta n_\theta) \tag{2}$$

[u_0 is the limiting velocity of shell projection calculated by Eq. (1)]. These dependences involve structural characteristics that exert the most significant effect on the parameters of explosive projection of the liquid and the shell. The coefficients $F_1 = 1.035$ and $G_1 = 0.395$ define the distributions for the basic model ($R_0 = 11$ mm, $a_0 = 20$ mm, and

$b_0 = 26.7$ mm; 36/64 TNT/RDX explosive with water as a filler; shell material is steel; $n_\theta = 16$ and $a_f/a_0 = 1.4$), and the remaining coefficients determine the difference of a particular model from the basic model due to variation of one parameter.

Based on the calculated results, we found the following analytical dependences that provide a physically adequate description of the influence of each parameter on the above-given distributions:

$$F_2 = 0.56 + 0.44\exp\left(4.5(1 - 0.55a_0/R_0)\right), \qquad G_2 = 1.37\beta/(0.028 + \beta),$$

$$F_3 = 1.72 - 0.72\rho_l/\rho_{\mathrm{H_2O}}, \qquad G_3 = 0.71 + 0.29\rho_p/\rho_{\mathrm{Fe}},$$

$$F_4 = 0.32 + 0.68\exp\left(2.2(1 - n_\theta/16)\right), \qquad G_4 = 1.5 - 0.5\rho_l/\rho_{\mathrm{H_2O}},$$

$$F_5 = 1.069[1 + 0.069\exp\left(-7(1.4 - a_f/a_0)\right)]^{-1}, \qquad G_5 = 1.2[1 + 0.2\exp\left(-5.8(1.4 - a_f/a_0)\right)]^{-1}.$$

The shell thickness is not directly involved into the expressions for the coefficients of distributions (2), but it affects the load factor and, through the load factor, the number of sectors and the radius of shell fracture. Deriving an explicit dependence of the number of fragments on the shell thickness requires additional experiments on fracture of shells of different thicknesses under the action of HE charges through a liquid layer.

As the systems of differential equations for the shell, liquid, and detonation products admit their recording in a dimensionless form, Eqs. (2) can be used for geometrically similar models of different scales.

REFERENCES

1. V. I. Stikachev, *Creation of a Protective Medium in Explosion-Related Operations* [in Russian], Nauka, Moscow (1972).
2. N. E. Umnov, A. S. Golik, D. Yu. Paleev, et al., *Prevention and Localization of Explosions in Underground Conditions* [in Russian], Nedra, Moscow (1990).
3. P. G. Kachurin, *Physical Basis for Affecting Atmospheric Processes* [in Russian], Gidrometeoizdat, Leningrad (1973).
4. B. W. Smith, W. B. Richardson, D. W. Parkinson, and E. Lee Helms, "Liquid or foam fire retardant delivery device with pyrotechnic actuation and aeration," U.S. Patent No. 6371213, MPK^7 A 62 S 11/00, Publ. 04.16.02; NKI 169-73.
5. A. E. Kolobanova, V. A. Odintsov, and L. A. Chudov, *Propagation of a System of Cracks in a Cylinder under Pulsed Loading* [in Russian], Inst. Problems Mechanics, Moscow (1981).
6. M. L. Wilkins, "Calculation of elastoplastic flows," in: B. Alder, S. Fernbach, and M. Retenberg (eds.), *Methods of Computational Physics*, Vol. 3, Academic Press, New York (1964).
7. L. P. Orlenko (ed.), *Physics of Explosion* [in Russian], Fizmatlit, Moscow (2004).
8. K. P. Stanyukovich, *Unsteady Motion of Continuous Media*, Pergamon Press, New York (1960).
9. A. V. Kashirskii, L. P. Orlenko, and V. N. Okhitin, "Effect of the equation of state on the dispersion of detonation products," *J. Appl. Mech. Tech. Phys.*, **14**, No. 2, 286–290 (1973).
10. A. V. Kashirskii, Yu. V. Korovin, and L. A. Chudov, "Explicit difference method for calculating two-dimensional unsteady problems of motion of detonation products," in: *Computational Methods and Programming* (collected scientific papers) [in Russian], No. 19, Izd. Mosk. Univ., Moscow (1972), pp. 97–107.
11. V. A. Bykov, E. F. Gryaznov, and V. N. Okhitin, "Explosive projection of a shell through a liquid layer," *Oboron. Tekh.*, Nos. 9/10, 21–25 (1999).
12. V. A. Odintsov and T. G. Statsenko, "Fracture of cylinders at the wave stage," *Izv. Akad. Nauk SSSR, Mekh. Tverd. Tela*, No. 2, 56–62 (1980).
13. E. F. Gryaznov, E. V. Karmanov, V. V. Selivanov, et al., "Morphology of fracture of cylindrical shells at the wave stage," *Probl. Prochn.*, No. 5, 89–91 (1984).
14. A. E. Kolobanova, "Calculation of the number of cracks and their size distribution in the case of pulsed viscous fracture of a ring," *Probl. Prochn.*, No. 9, 73–79 (1989).
15. A. E. Kolobanova and V. V. Selivanov, *Fundamentals of Shell Fracture Dynamics. Educational Aid* [in Russian], Bauman Moscow State Techn. Univ., Moscow (1996).
16. P. G. Tomilov, V. N. Okhitin, E. F. Gryaznov, et al., "Deformation and fracture of steel shells under pulsed loading through a liquid layer," in: *Dynamic Strength and Crack Resistance of Structural Materials*, Proc. Rep. Workshop, Kiev Higher Tank Engineering School, Kiev (1988), pp. 185–190.